Journal Pre-proofs

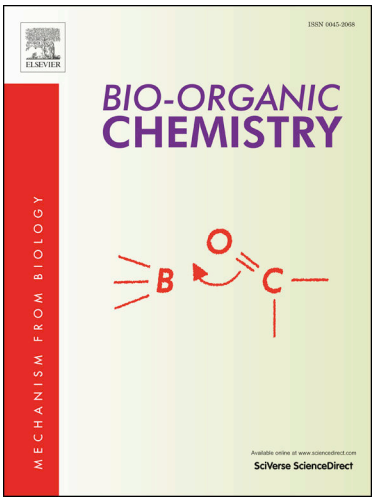

Symmetric benzidine derivatives as anti-HCV agents: insight into the nature, stereochemistry of the capping amino acid and the size of the terminal capping carbamates

Shereen E. Abdel Karim, Youssef H. Youssef, Mohammad Abdel-Halim, Efseveia Frakolaki, Niki Vassilaki, Grigoris Zoidis, Nermin S. Ahmed, Ashraf H. Abadi

PII: S0045-2068(20)31386-9
DOI: https://doi.org/10.1016/j.bioorg.2020.104089
Reference: YBIOO 104089

To appear in: *Bioorganic Chemistry*

Received Date: 4 March 2020
Revised Date: 30 June 2020
Accepted Date: 7 July 2020

Please cite this article as: S.E. Abdel Karim, Y.H. Youssef, M. Abdel-Halim, E. Frakolaki, N. Vassilaki, G. Zoidis, N.S. Ahmed, A.H. Abadi, Symmetric benzidine derivatives as anti-HCV agents: insight into the nature, stereochemistry of the capping amino acid and the size of the terminal capping carbamates, *Bioorganic Chemistry* (2020), doi: https://doi.org/10.1016/j.bioorg.2020.104089

Symmetric benzidine derivatives as anti-HCV agents: insight into the nature, stereochemistry of the capping amino acid and the size of the terminal capping carbamates

Shereen E. Abdel Karim[a], Youssef H. Youssef[a], Mohammad Abdel-Halim[a], Efseveia Frakolaki[b], Niki Vassilaki[b], Grigoris Zoidis[c], Nermin S. Ahmed[a], Ashraf H. Abadi[a*]

[a]Faculty of Pharmacy and Biotechnology, Department of Pharmaceutical Chemistry, German University in Cairo, 11835 Cairo, Egypt.

[b]Molecular Virology Laboratory, Hellenic Pasteur Institute, Vas. Sofias Avenue, 11521, Athens, Greece.

[c]Department of Pharmacy, Division of Pharmaceutical Chemistry, School of Health Sciences, National and Kapodistrian University of Athens, GR-15771, Athens, Greece.

*Correspondence: Prof. Ashraf H. Abadi, Faculty of Pharmacy and Biotechnology, Department of Pharmaceutical Chemistry, German University in Cairo, 11835 Cairo, Egypt. Email: ahabadi@yahoo.com; ashraf.abadi@guc.edu.eg

Abstract

Novel symmetric molecules, bearing a benzidine prolinamide core, two terminal carbamate caps of variable sizes and nature, including natural and unnatural amino acids were developed. Several terminal *N*-carbamate substituents of the core structure, ranging from linear methyl, ethyl and butyl groups to branching isobutyl group; and an aromatic substituent were also synthesized.

Series 1 has hydrophobic AA residues, namely *S* and *R* phenylglycine and a terminal carbamate capping group, whereas Series 2 bears sulphur containing amino acids, specifically *S* and *R* methionine and the natural *R* methylcysteine. The novel compounds were tested for their inhibitory activity (EC_{50}) and their cytotoxicity (CC_{50}), using an HCV 1b (Con1) reporter replicon cell line. Compound **4** with the unnatural capping residue, bearing *D*-Phenylglycine amino acid residue and *N*-isobutyloxycarbonyl capping group, was the most active within the two series, with EC_{50}=0.0067 nM. Moreover, it showed high SI_{50} >14788524 and was not cytotoxic at the highest tested concentration (100 μM), indicating its safety profile. Compound **4** also inhibited HCV genotypes 2a, 3a and 4a. Compared to the clinically approved NS5A inhibitor Daclatasvir, compound **4** shows higher activity against genotypes 1b and 3a, as well as improved safety profile.

Keywords: NS5A inhibitors; Anti-HCV; capping groups.

1. Introduction

Hepatitis C is a hepatic disease induced by a blood borne virus called hepatitis C virus (HCV). The severity of hepatitis ranges from mild illness that can be cured within a few weeks, to a life-threatening disease, meanwhile 80% of the patients progress into a chronic infection [1]. Hepatitis C is a global health problem, as about 71 million people are infected chronically and at risk of cirrhosis, liver failure, and hepatocellular carcinoma. To date, there is no available vaccine for hepatitis C.

HCV belongs to family *Flaviviridae,* genus *Hepacivirus* [2] and it contains a positive sense single strand RNA with length of 9600 nucleotides that encodes around 3000 amino acids polyprotein.[3] The RNA polymerase of the virus is error-prone, so HCV shows high genetic variability and classified into seven main genotypes and more than 100 subtypes that vary regarding the risk factors of infections, response to treatment and geographic distribution [4].

The HCV genome consists of 5' and 3'- terminal non translated regions (5` and 3`-NTR) and a central open reading frame (ORF) which encodes a polyprotein processed into structural (S) proteins (core [C], E1 and E2) and non-structural (NS) proteins (p7, NS2, NS3, NS4A, NS4B, NS5A, and NS5B) [5,6]. NS5A is hydrophilic multifunctional phosphoprotein essential for HCV replication and assembly. Moreover, it modulates cell signaling pathways and the interferon response. Thus, NS5A is the target for current therapeutic strategies [7]. Until 2011, the standard therapy of HCV was Pegylated interferon-α combined with Ribavirin for a duration of 24 or 48 weeks [8,9]. In 2011, a breakthrough in the treatment of HCV was accomplished with the development of novel direct-acting antivirals (DAA) with pan-genotypic activity, high efficacy and less side effects [10].

DAAs are classified into three main classes: NS3/4A protease inhibitors, RNA-dependent RNA-polymerase NS5B inhibitors, and NS5A protein inhibitors [11]. The first clinically approved NS5A inhibitor was daclatasvir in 2014, followed by ledipasvir, ombitasvir, elbasvir, velpatasvir and pibrentasvir. Although these inhibitors have extremely high potency, their clinical application is still limited due to the high cost, their somewhat low efficacy against non-genotype 1 HCV strains and a tendency to develop drug resistance[12]. Recently, in 2019, several modifications were done to ombitasvir, the first generation NS5A inhibitor, where a dianiline or an aniline core was used together with natural and unnatural amino acids. These compounds show more selectivity toward GT 1b and 4a [13].

The efficacy of daclatasvir against the different HCV genotypes varies, with genotype 3 being the least sensitive [14]. Only the recently approved pibrentasvir and velpatasvir show similar activity against all HCV genotypes [12]. As genotype 3 represents 30% of HCV infections worldwide [15], there is still an urgent need for the development of more potent pan-genotypic NS5A inhibitors with significant activity against genotype 3.

Different studies revealed the dimeric nature of domain I of NS5A and represented a significant advance in the study of NS5A replication complex inhibitor (NS5A RCI)−target interactions [16]. The roughly symmetrical nature of the most active NS5A inhibitors and the symmetry of the crystallized protein dimer complements are consistent with resistance-associated mutations suggesting that domain I is the binding site of daclatasvir and structurally related compounds.

Our research group have recently worked on the design of symmetrical NS5A inhibitors. [13, 17] Symmetrical analogues bearing a benzidine core were moderately active. [17] During the course of our work, some monomeric benzidine analogues were prepared and tested, they showed

no significant anti-HCV activity on CON-1, Genotype 1b when compared to their symmetric congeners. For example (diethyl ((2S,2'S)-((2S,2'S)-(([1,1'-biphenyl]-4,4' diylbis (azanediyl))bis(carbonyl))bis(pyrrolidine-2,1-diyl))bis(3-methyl-1-oxobutane-1,2-diyl))dicarbamate), compound 9, reference 17, EC_{50} 13.9 μM, versus (ethyl ((S)-3-methyl-1-oxo-1-((S)-2-((4'-((S)-pyrrolidine-2-carboxamido)-[1,1'-biphenyl]-4-yl)carbamoyl)pyrrolidin-1-yl)butan-2-yl)carbamate) EC_{50} >20 μM. This same finding was observed with other cores we investigated (Abadi et al, unpublished data).

Therefore, we turned our attention only to this class of symmetric benzidine compounds. Our aim was to expand the chemical space around this promising core and to develop potent pan genotypic analogues with high safety margin.

In this study, symmetric NS5A inhibitors with benzidine *L*-prolinamide core, natural, unnatural and sulphur-containing amino acids, were designed and synthesized. The key pharmacophoric features of other reported NS5A inhibitors, such as the two hydrophobic aromatic regions, a terminal hydrophobic chain and two or more hydrogen bond acceptors were maintained [24] (Fig. 1).

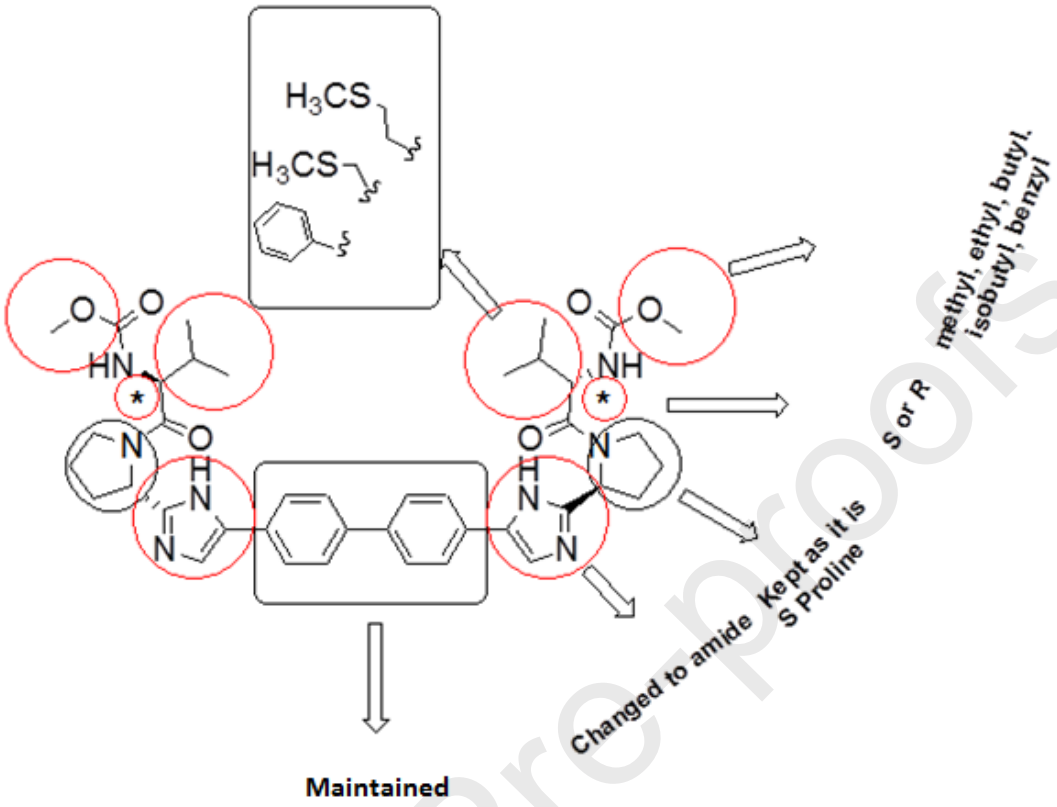

Fig.1. Structural changes performed on the clinically approved NS5A inhibitor **daclatasvir** to obtain compounds **1-25**.

2. Results and discussion

2.1. Chemistry

Amide coupling of benzidine with *N*-Boc-*L*-Proline using coupling reagent EEDQ led to *N*-Boc-protected compound, followed by deprotection with triflouroacetic acid (TFA) to give the free amine, as (outlined in Scheme 1). Two series of capping groups were synthesized. The first series **1-10** were synthesized by the reaction of *D, L*- phenylglycine and the corresponding chloroformate in NaOH yielding the respective carbamate derivatives (outlined in Scheme 2). The

second series were synthesized by the reaction of sulphur containing amino acids (*D, L*-methionine **11-20** and alkylated *L*-cysteine **21-25** respectively with the corresponding chloroformate yielding the respective carbamate derivatives (outlined in Scheme 3 and 4). Coupling each of these carbamate derivatives to the free amine using HBTU as a coupling reagent was done (outlined in Scheme 1). The carbamate terminal groups varied from non-branching to branching alkyl chains and from aliphatic to aromatic groups.

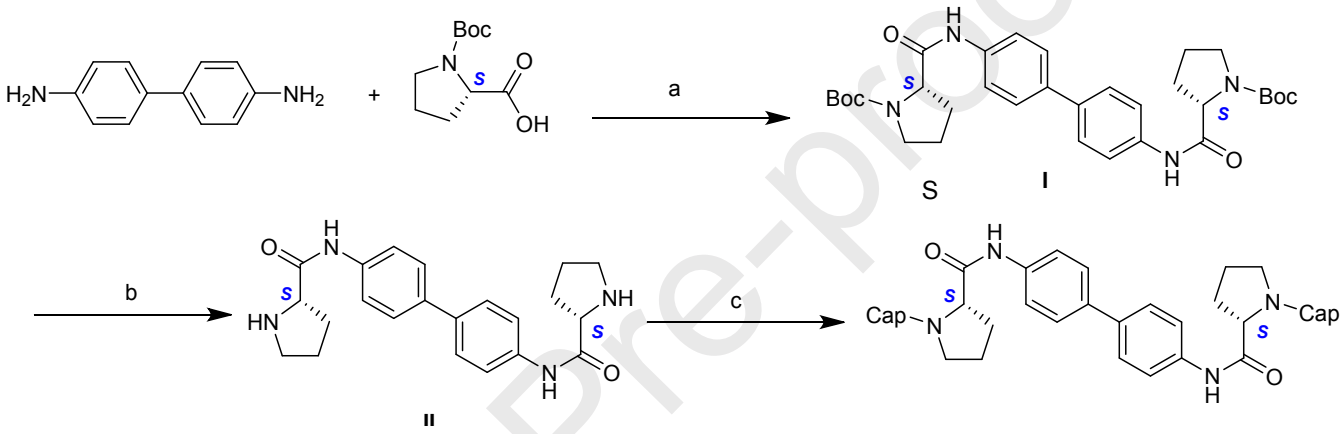

Scheme 1. Reagents and Conditions: (a) N-Boc-L-Proline, EEDQ, CH_2Cl_2, 94%; (b) TFA, CH_2Cl_2; (c) capping group (CG1-25), HBTU, DIPEA, CH_2Cl_2, 21-38%.

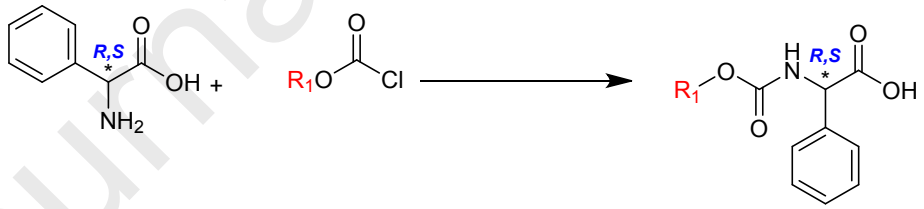

For exact R, R_1 and configuration of the capping AA, see Table 1

Scheme 2. Reagents and Conditions: aqueous NaOH, Dioxane.

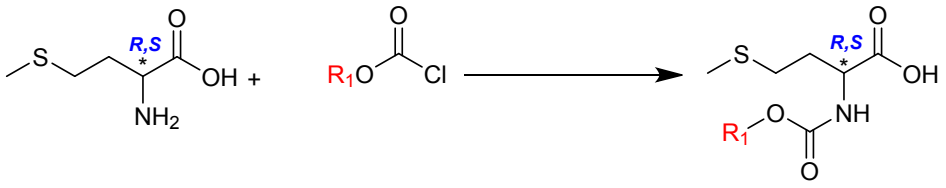

For exact R_1 and configuration of the capping AA, see Table 1

Scheme 3. Reagents and Conditions: Aqueous NaOH, Dioxane.

Finally, we also prepared thioether derivatives of *L*-Cysteine *via S*-alkylation to *S*-methyl in good yield under basic conditions using 1,1,3,3-tetramethyl guanidine (TMG).

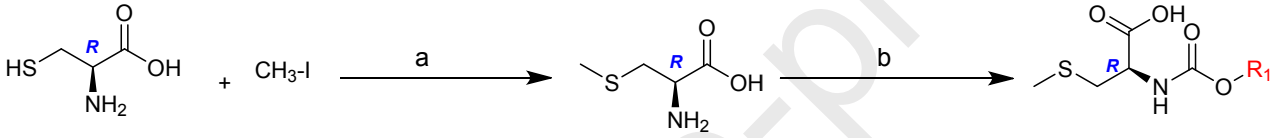

For exact R_1 and configuration of the capping AA, see Table 1

Scheme 4. Reagents and Conditions: (a) TMG, MeOH, Argon, 50°C; (b) Aqueous NaOH , Chloroformates, Dioxane.

The molecular masses and purity of the synthesized compounds were confirmed using LC/MS. The charts of the compounds show molecular ion peak appear at $(M+H)^+$, in addition to a peak with m/z ratio half that of the molecular ion peak due to the symmetrical structures of the compounds.

2.2. Compound screening against HCV genotype 1b replicon

Two series of novel dimeric analogues were synthesized. **Series 1** has hydrophobic AA residues and a terminal carbamate capping group, whereas **Series 2** bears sulphur-containing amino acids. The latter molecules have been designed to be active in their original form, as it has been reported that they have the potential to be metabolized intracellularly via CYP450 to

sulfoxide and sulfone moieties, which have anti-HCV activity [25]. This synthetic approach could possibly lead to a complementary resistance profile. The residues bear *N*-methoxycarbonyl, *N*-ethoxycarbonyl, *N*-butyloxycarbonyl, *N*-isobutyloxycarbonyl or *N*-benzyloxycarbonyl carbamates as terminal capping groups.

Compounds were tested for their effect on HCV RNA replication and cell viability in the stable cell line Huh5-2 bearing a reporter replicon of HCV genotype 1b (strain Con1) [26]. In this system, the level of viral replication corresponds to the level of the co-expressed firefly luciferase. Cells were treated with serial dilutions of the compounds in cell culture medium for 72 hours, where the final concentration of the solvent DMSO was 0.2%, so as not to affect viral replication levels (data not shown). The activity (expressed as the 50% effective concentration [EC_{50}]) and the cytotoxicity (expressed as the 50% cytotoxic concentration [CC_{50}]) of compounds **1**-**25** were calculated by measuring luciferase activity derived from HCV replication and intracellular ATP levels, respectively. The selectivity index (SI_{50}) was calculated as ratio of CC_{50} versus EC_{50}. The results are summarized in (Table 1) and dose-response curve analysis for the most potent analogues is presented (Fig. 2), using Daclatasvir as positive control.

The benzidine *L*-prolinamide part is contained in all 25 compounds. Although most of the commercially available NS5A inhibitors bear *L*-valine methyl carbamate ester as a capping group, in our approach we adopted different capping groups of *D, L*-phenylglycine, *D, L*-methionine or alkylated *L*-cysteine with different alkyl/aryl carbamate esters, which were designed to have higher inhibitory activity.

Series 1 consists of carbamate derivatives with different capping groups that vary in length, branching and aromaticity. It is worth mentioning that incorporation of a phenylglycine group on both caps, show high inhibitory activities, regardless of the type of carbamate ester. Compounds

1-10 showed the highest potency among all analogues tested, with EC_{50} 0.0067- 30 nM. This indicated that the lipophilic features are essential for interaction with the nearby lipophilic residues of NS5A and for better binding affinity for the target protein.

Compound **4** was the most active compound within the two series, with EC_{50}=0.0067 nM. Moreover, it showed high SI_{50} >14788524 and was not cytotoxic at the highest tested concentration (100 μM), indicating its safety profile. It bears *D*-phenylglycine amino acid residue and *N*-isobutyloxycarbonyl capping group. We conclude that these features are essential for interactions with the receptor.

Surprisingly, within **Series 1** compounds **1-5** and **6-10**, containing the amino acid phenylglycine, the *D*-epimers **1-5** showed the highest activity. This highlights the importance of testing both natural and unnatural epimers of the same residue to figure out the more potent derivatives and emphasizes the crucial role of the stereocenter of the amino acids.

Concerning the carbamate moiety in the *D*-phenylglycine containing molecules **1-5**, we observed that compounds **4** and **5** that bear an *N*-isobutyloxycarbonyl and *N*-benzyloxycarbonyl capping group, respectively, were the most active, with EC_{50}= 0.0067 nM and 0.018 nM. This indicates that, in this series, the presence of aromatic or bulkier alkyl capping groups confers higher activity rather than the small aliphatic ones.

Among *L*-phenylglycine carbamate derivatives **6-10**, compound **10**, bearing an *N*-benzyloxycarbonyl capping group, was the most active one with EC_{50}= 0.3 nM. This indicates that aromaticity is essential for interactions with the target protein for this series of compounds.

In **Series 2**, a new approach was adopted. Instead of the commonly used lipophilic AA residues, we investigated the role of sulphur containing AA namely *D, L*-methionine and *L*-cysteine in the capping groups.

Among compounds **11**-**20** of **Series 2**, bearing a methionine amino acid residue**,** compound **18**, with a *N*-butyloxycarbonyl group, was the most active analogue with EC_{50}= 31.27 nM and SI_{50}>3198. However, upon comparing the rest of the *S*-epimers (*L*-methionine amino acids) to the *R*- epimers (*D*-methionine amino acids) of the synthesized analogues, it was observed that the *R*-epimers were more potent, confirming the importance of the stereocenter of the AA residue and the crucial role of the projection plane for compound activity. These results expand the chemical space from which new NS5A inhibitors can be discovered.

Among analogues **21**-**25** of **Series 2**, containing a *S*-methyl *L*-cysteine AA residue, compound **21**, that bears a *N*-methoxycarbonyl capping group, was the most active with EC_{50}=33.87 nM and SI_{50}>2952. This indicates that for the analogues in this series, less bulky aliphatic capping groups confer higher efficacy.

Interestingly, upon comparing the EC_{50} of *L*-cysteine compounds **21**-**25** with the respective ones for methionine-bearing compounds **11**-**15**, we noticed that compound **21** showed better activity (EC_{50}= 33.87 nM) relative to compound **11** (EC_{50}= 443.1 nM), while the rest of methionine derivatives **12**-**15**, with EC_{50}= 83 -508 nm, were more potent than compounds **22**-**25**. This suggests that the overall features of the molecule determine the anti-HCV efficacy.

Table 1: Activity, cytotoxicity and selectivity of the synthesized compounds (1-25) in HCV genotype 1b (Con1) replicon assay.

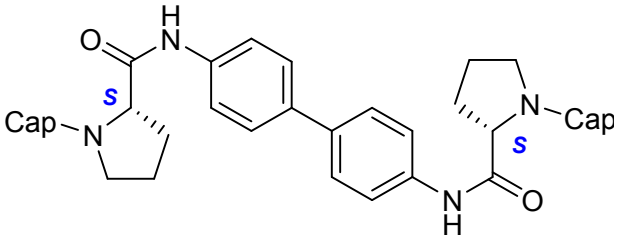

Cpd #	Capping groups	Stereochemistry	EC_{50}(nM)	CC_{50}(nM)	SI_{50}
1	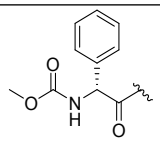	*R*	0.0568	92510	1628697
2	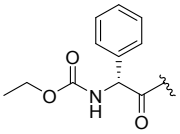	*R*	0.03954	>100000	>2529084
3	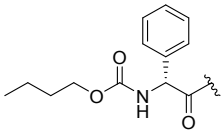	*R*	0.08061	>100000	>1240541
4	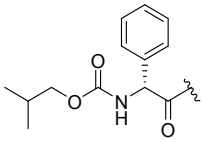	*R*	0.006762	>100000	>14788524
5	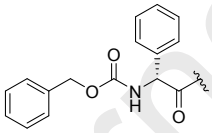	*R*	0.01838	35330	1922198
6	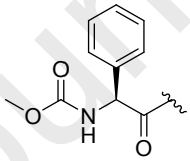	*S*	4	>10000	>2500
7	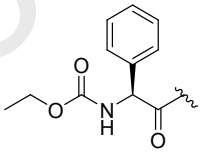	*S*	4	>2500	>625
8	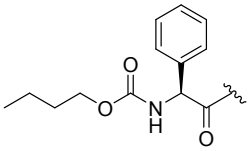	*S*	30	>10000	>333

9	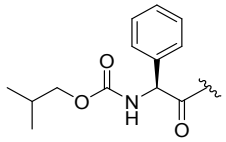	*S*	30	>10000	>333
10	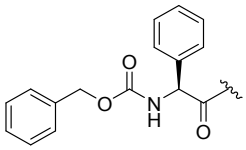	*S*	0.32	88180	274618
11	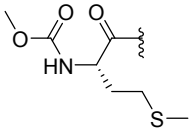	*R*	443.1	>100000	>226
12	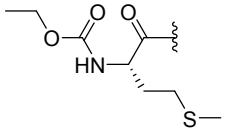	*R*	383.2	>100000	>261
13	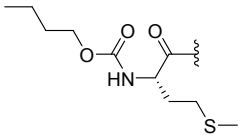	*R*	114.3	>100000	>875
14	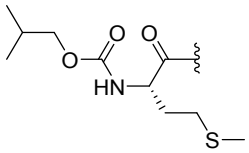	*R*	83.68	53740	642
15	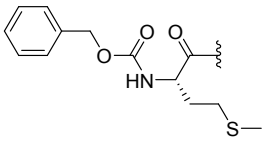	*R*	508.1	58140	114
16	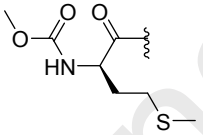	*S*	192.6	>100000	>519
17	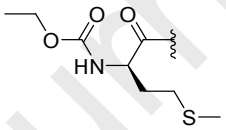	*S*	>1000	>1000	1
18	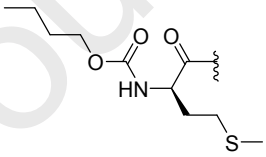	*S*	31.27	>100000	>3198
19	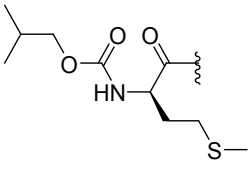	*S*	>1000	>1000	1

20	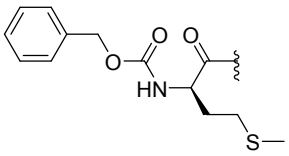	*S*	>1000	>1000	1
21	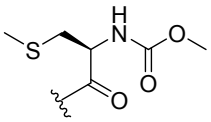	*R*	33	>100000	>2952
22	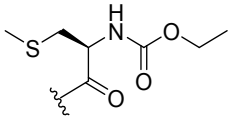	*R*	>1000	>1000	1
23	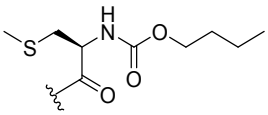	*R*	>1000	>1000	1
24	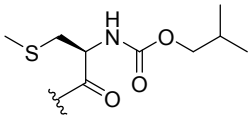	*R*	>1000	>1000	1
25	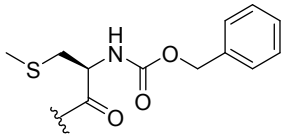	*R*	>1000	>1000	1
	Daclatasvir		0.0197	17700	898477

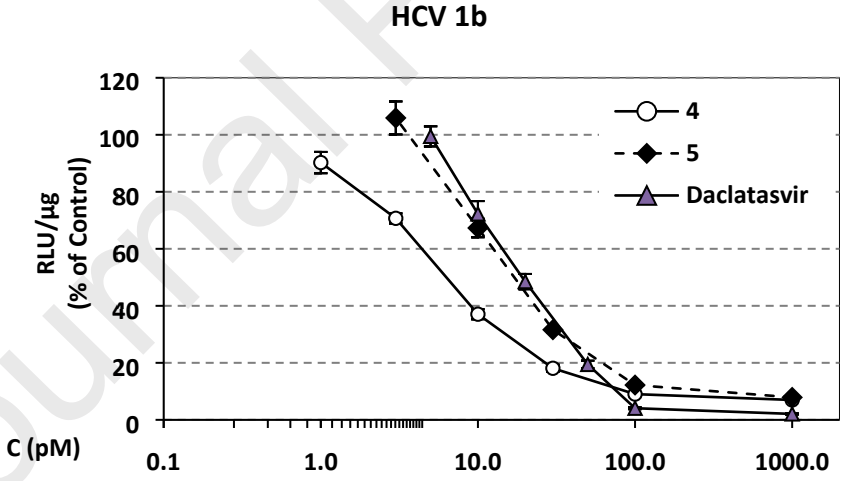

Fig. 2. Dose–response curve analysis for compounds **4** and **5** against HCV genotype 1b RNA replication. Serial dilutions of the compounds were used to treat for 72 h Huh5-2 subgenomic replicon cells seeded at 30% confluency. Viral RNA replication-derived firefly luciferase activity was determined and expressed as relative light units (RLU) per µg of total protein. Values from cells treated with the solvent DMSO (control) were set to 100%. Daclatasvir was used as a positive control. Bars represent mean values obtained from three separate experiments in triplicate. Error bars represent standard deviation (SD).

2.3. Activity of compounds 4 and 5 against other HCV genotypes

Compounds **4** and **5** from **Series 1**, exhibiting the highest potency against HCV genotype 1b among all synthesized compounds, were tested against other HCV genotypes. The effect of the compounds on viral replication-derived luciferase activity was examined in Huh7-JFH1, Huh7.5-3a and Huh7.5-4a stable cell lines containing subgenomic replicons of HCV GT 2a (strain JFH1), GT 3a (strain S52) and GT 4a (strain ED43), respectively. The clinically approved NS5A inhibitor **daclatasvir** was used for comparison.

Between the two molecules, compound **4** was more potent than compound **5** in all genotypes tested (Table 2). Specifically, compound **4** showed significant activity against genotype 3a, with EC_{50} 1.365 nM. In addition, its activity against genotype 2a was slightly lower but still very strong, with EC_{50}=5.183 nM. Concerning genotype 4a, compound **4** had EC_{50}=142.2 nM. It is worth mentioning that the low cytotoxicity of the compound, in combination with its significant activity in genotypes 2a and 3a, resulted in SI_{50} more than 5 orders of magnitude. Thus, compound **4** shows high efficiency and against genotypes that are difficult to treat. Interestingly, compared to daclatasvir, compound **4** was ~6 times more active in genotype 3a, while it also exhibited significantly less cytotoxicity.

Table 2: Activity, cytotoxicity and selectivity of compounds **4** and **5**, compared to **Daclatasvir**, HCV genotype 1b (Con1), 2a (JFH1), 3a (S52) and 4a (ED43) replicon assays.

Genotype		**GT 1b**		**GT 2a**		**GT 3a**		**GT 4a**	
	CC_{50} (nM)	**EC_{50} (nM)**	**SI**	**EC_{50} (nM)**	**SI**	**EC_{50} (nM)**	**SI**	**EC_{50} (nM)**	**SI**
4	>100000	0.006762	>14788524	5.183	>19294	1.365	>73260	142.2	>703
5	35330	0.01838	1922198	38.127	927	2.275	15530	273.0	129
Daclatasvir	17700	0.01965	900763	0.05784	306017	8.348	2120	0.02119	835300

2.4. Effect of compound 4 on HCV RNA and protein levels

To confirm the anti-HCV activity of compound **4** and its mechanism of action by additional assays other than measuring the virus-derived luciferase levels, viral HCV RNA and NS5A protein levels in genotype 1b replicon cells (Huh5-2) were determined. Cells were treated with serial dilutions of the compound and then viral RNA was quantified using reverse transcription - quantitative polymerase chain reaction (RT-qPCR) and NS5A was evaluated using indirect immunofluorescence**.** DMSO-treated cells were used as a negative control. We observed that compound **4** reduced HCV RNA replication (Fig. 3A) with EC_{50}=0.0089 pM, consistently to the decrease in replication-derived luciferase activity (Table 1). In agreement, HCV NS5A levels, as shown by indirect immunofluorescence analysis in replicon cells, were significantly reduced in the highest compound concentration used (Fig. 3B).

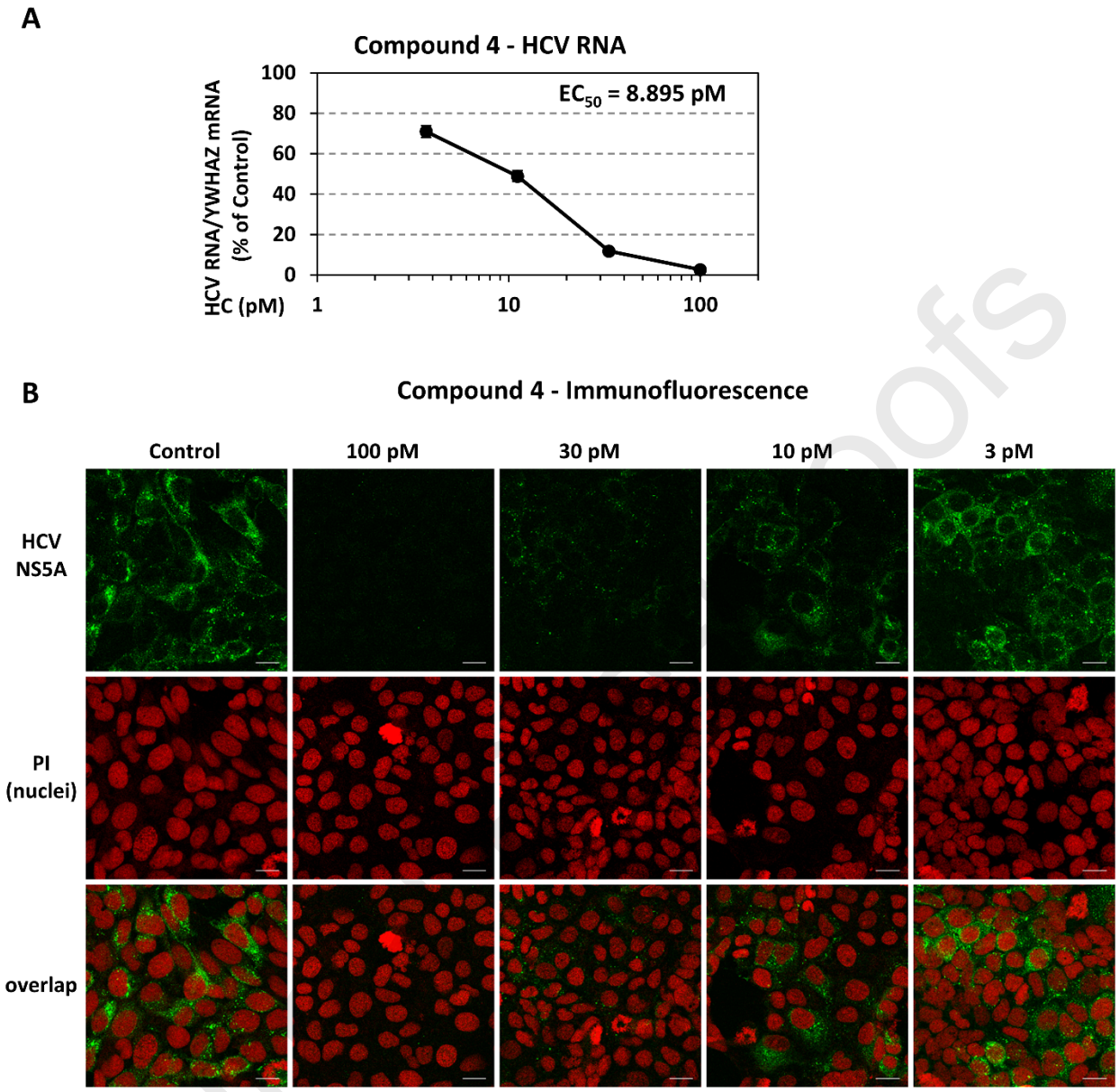

Fig. 3. Effect of compound **4** on HCV RNA and protein expression levels in a subgenomic HCV genotype 1b (Con1) replicon assay. Huh5-2 replicon cells were treated with serial dilutions of compound **4** or the solvent DMSO, for 72 hours. (**A**) (+) strand HCV RNA was quantified by RT-qPCR and normalized to the mRNA levels of the housekeeping gene YWHAZ (tyrosine 3-monooxygenase/tryptophan 5-monooxygenase activation protein zeta). Values from cells that were treated with DMSO (control) were set to 100. (**B**) HCV NS5A staining (left column), using indirect immunofluorescence. Nuclei were stained with propidium iodide (PI; middle panels) as a cell viability marker. Merged images are shown at the right. Scale bar, 20 μm.

2.5. Combinatory effect of compound 4 with DCV

To examine the interaction of compound **4** in combination with an approved NS5A inhibitor, Huh5-2 replicon cells were treated with compound **4** in the presence or absence of daclatasvir (DCV). Compound **4** and DCV had an antagonistic effect, which was determined by calculating the coefficient of drug interaction (CDI≈1.3). This indicates that both compounds bind at the same site in NS5A (Fig 4).

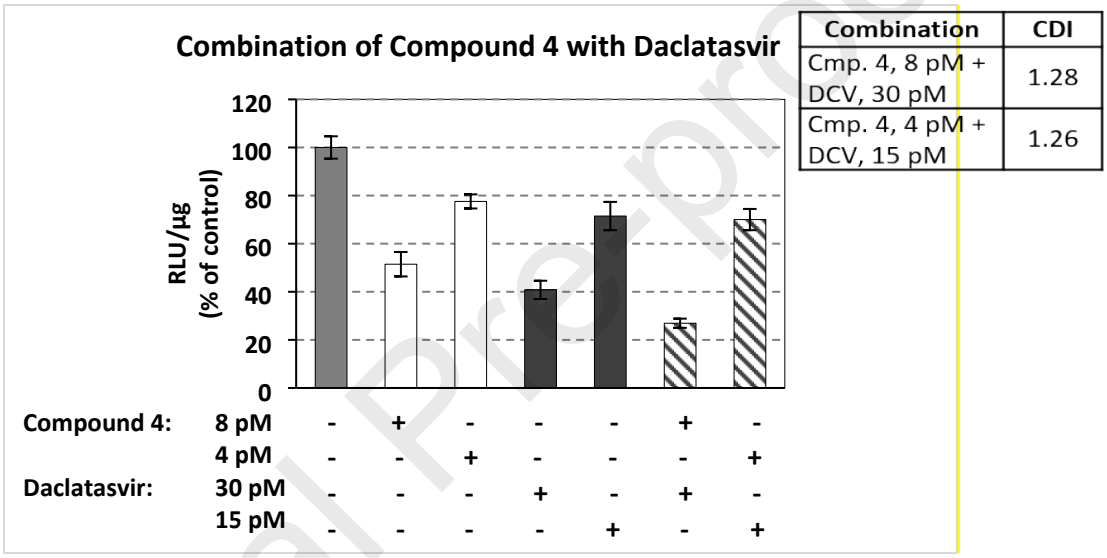

Combination	CDI
Cmp. 4, 8 pM + DCV, 30 pM	1.28
Cmp. 4, 4 pM + DCV, 15 pM	1.26

Fig. 4. Combinatory activity of compound **4** (Cmp. 4) with Daclatasvir (DCV) against HCV replication. Huh5-2 cells were treated or not with 30 pM or 15 pM DCV in the presence or absence of compound **4**. F-Luc activity was determined and calculated as relative light units (RLU) per µg of total protein. Values were expressed as percentage of those obtained with cells treated with the solvent DMSO (control). CDI: coefficient of drug interaction, CDI=AB/(AxB). Bars represent mean values obtained from three separate experiments in triplicate. Error bars represent standard deviation (SD).

3. Conclusions

Despite the challenges that the discovery of pan-genotypic HCV NS5A inhibitors has to face, due to the significant diversity among mutants/genotypes and the absent of protein/inhibitor complexes X-ray structures for rational inhibitor design, we discovered a potent and almost pan-

genotypic NS5A inhibitor. Compound **4** with the unnatural capping residue, bearing *D*-Phenylglycine amino acid residue and *N*-isobutyloxycarbonyl capping group, was the most potent within the two series against genotype 1b, highlighting that these features are essential for interactions with the receptor. These results expand the chemical space from which new NS5A inhibitors may be discovered. Compound **4** inhibited HCV genotypes 2a, 3a and 4a, with significant activity against genotype 3a with EC_{50} 1.365 nM. Concerning genotype 4a, which is the most prevalent in Egypt, compound **4** had EC_{50} 142.2 nM. It is noteworthy that compound **4** compared to **daclatasvir** proved to be 16 and 35 more active against genotypes 1b and 3a respectively. Results of combinatory effect of compound **4** and DCV indicate that both compounds bind at the same site in NS5A.

Our findings suggest that the novel symmetric molecules, bearing a benzidine prolinamide framework that we have developed, following mild and experimentally convenient protocols, offers a promising core for further construction of new analogues with two terminal carbamate caps of variable sizes and nature endowed with optimized anti-HCV properties through appropriate terminal N-carbamate substituents. Future experiments with asymmetric scaffolds and further modifications on the rigid biphenyl core should deliver more detailed SAR information to help refine the requirements for optimal NS5A inhibitory activity.

4. Experimental section

4.1. Chemistry

All starting materials, organic solvents and reagents were obtained from commercial suppliers and used without purification. Column chromatography carried out using silica-gel 70-230 μM mesh. The progress of the reactions was monitored by TLC using fluorescent pre-coated silica gel plates and the compounds were detected by short UV light (λ= 254 nm). Reactions were performed under argon when inert atmosphere was required. The detection of carbamates was done using furfural/sulphuric acid solution.

^{1}H-NMR spectra were done on Varian spectrometer, at 400 MHz and ^{13}C-NMR spectra were run at 101 MHz in Dimethyl Sulfoxide (DMSO). Chemical shifts (δ) were reported in parts per million (ppm) downfield from TMS; and all coupling constants (*J*) were given in Hz. The purities of the compounds were detected by HPLC coupled with mass spectrometer and were more than 90% for all compounds.

The Mass spectrometric analysis (UPLC-ESI-MS) was carried out using Waters ACQUITY XevoTQD system, which consisted of an ACQUITY UPLC H-Class system, Xevo^{TM} TQD triple-quadrupole tandem mass spectrometer and an electrospray ionization (ESI) interface (Waters Corp., Milford, MA, USA). Acquity BHE C_{18} 100mm x 2.1 mm column (particle size, 1.7 μm was used to separate analytes (Waters, Ireland). The solvent system was composed of water containing 0.1% TFA in acetonitrile (B). The masses were reported as protonated ions $(M+H)^{+}$.

4.1.1. General procedures for the preparation of capping groups CG 1-20 *[27]*

A 500 mL round bottom flask was equipped with a magnetic stir bar, charged with distilled H_2O (100 mL) and NaOH (100 mmol, 4.0 g) and cooled in an ice bath to 0 °C. *L*-Phenylglycine/*L*-Methionine/*D*-Phenylglycine/*D*-Methionine (35 mmol) was added, and stirred until the solution was homogeneous. The corresponding carbonyl chloride (45.5 mmol) in 1,4-dioxane (40 mL) was added dropwise using an addition funnel. The reaction mixture was left to stir overnight at room temperature. The solution was extraction of the solution with Et_2O (3 × 50 mL) was done, and the organic layers were discarded. The aqueous layer was cooled in an ice bath to 0 °C, and concentrated HCl was added dropwise until the pH = 2. The re-extraction of the aqueous solution was done with Et_2O (3 × 100 mL). The organic layers were combined, dried over anhydrous $MgSO_4$, filtered, and concentrated *in vacuum* to give the product as clear viscous oil. No further purification was required.

4.1.2. General procedures for the preparation of alkylated L-Cysteine *[28]*

A solution of 1,1,3,3-tetramethyl guanidine (21 mmol) in 5 mL of MeOH was added dropwise to a previously stirred mixture (under argon) of *L*-Cysteine (10 mmol) in 10 mL of MeOH. To the homogenous reaction mixture was added alkylation reagent methyl iodide (10 mmol) in tetrahydrofuran dropwise and then was stirred for 1 h at 50°C. Then 10 mL of H_2O acidified with a stoichiometric quantity of AcOH (1:1) was added. The separated precipitate by vacuum filtration was washed several times with ethanol to give white/off white solid. No further purification was required.

4.1.3. General procedures for the preparation of capping groups CG 21-25 [27]

A 500 mL round bottom flask was equipped with a magnetic stir bar, charged with distilled H_2O (100 mL) and NaOH (100 mmol, 4.0 g) and cooled in an ice bath to 0 °C. *S*-methyl cysteine (35 mmol) was added, and stirred until the solution was homogeneous. The corresponding carbonyl chloride (45.5 mmol) in 1,4-dioxane (40 mL) was added dropwise using an addition funnel. The reaction mixture was left to stir overnight at room temperature. The solution was extraction of the solution with Et_2O (3 × 50 mL) was done, and the organic layers were discarded. The aqueous layer was cooled in an ice bath to 0 °C, and concentrated HCl was added dropwise until the pH = 2. The re-extraction of the aqueous solution was done with Et_2O (3 × 100 mL). The organic layers were combined, dried over anhydrous $MgSO_4$, filtered, and concentrated *in vacuum* to give the product as clear viscous oil. No further purification was required.

4.1.4. General procedure for the preparation of (2S,2'S)-di-tert-butyl 2,2'-(([1,1'-biphenyl]4,4'diylbis(azanediyl))bis(carbonyl)) bis(pyrrolidine-1-carboxylate) (N-protected benzidine prolinamide) (I) [29]

EEDQ (22.58 g, 91.3 mmol) was added in one portion to a solution of benzidine (8.00 g, 38.1 mmol) and *N*-Boc-*L*-proline (18.83 g, 87.5 mmol) in dry CH_2Cl_2 (250 mL) and it was left to stir for 16 hours at room temperature under argon. The resultant component was removed *in vacuum*. The crude product was washed with Et_2O and vacuum-filtered to provide compound **I** as off white solid with 94% yield. No further purification was required.

4.1.5. General procedure for the preparation of (2S,2'S)-N,N'-([1,1'-biphenyl]-4,4'-diyl)bis(pyrrolidine-2-carboxamide) (Deprotected benzidine prolinamide) (II) *[29]*

CF_3CO_2H (60 mL) was added to the stirred solution of compound **I** (23.62 g, 40 mmol) in CH_2Cl_2 at room temperature under argon. The mixture was left to stir for 3 hours before additional portion of CF_3CO_2H (24 mL) was added. After stirring for an additional 4 hours at room temperature, the component was evaporated *in vacuum*. The residue was dissolved in EtOAc, washed with saturated $NaHCO_3$ solution and brine. 1 N NaOH was added until pH= 12. The residue was dried over anhydrous MgSO4 and concentrated *in vacuum* to give a pale yellow sticky solid, which was dissolved in acetone and evaporated *in vacuum*. This step was repeated 2-3 times to give pale yellow crystals. No further purification was required.

4.1.6. General procedure for the preparation of compounds 1-25 *[30]*

Capping groups **CG 1-25** (3 mmol) were added to compound **II** (0.4 g, 1 mmol), HBTU (1.13 g, 3 mmol) and TEA (0.7 mL) in CH_2Cl_2. The reaction mixture was left to stir for 2 hours under argon at room temperature. The solvent was removed *in vacuum* and then the residue was purified using silica gel column chromatography (98.5:1.5 CH_2Cl_2/ MeOH) to give compounds **1-25**.

4.1.6.1. Dimethyl ((1R,1'R)-((2S,2'S)-(([1,1'-biphenyl]-4,4'-diylbis(azanediyl))bis(carbonyl))bis(pyrrolidine-2,1-diyl))bis(2-oxo-1-phenylethane-2,1-diyl))dicarbamate (1)

Yellow semi-solid; yield: 29%; $C_{42}H_{44}N_6O_8$; LC/MS: $[M+H]^+$ = 761.32; purity 100%; ^{1}H-NMR (400 MHz, DMSO) δ 7.69 – 7.60 (m, 9H), 7.43 – 7.32 (m, 9H), 5.49 (s, 2H), 4.56 – 4.37 (m, 2H), 3.53 (t, J = 3.7 Hz, 4H), 3.35 (s, 6H), 2.16 – 1.82 (m, 8H); ^{13}C-NMR (101 MHz, DMSO)

δ 170.66, 168.55, 165.03, 156.77, 138.64, 137.34, 134.83, 129.03, 128.46, 126.85, 119.88, 61.00, 57.05, 51.98, 47.32, 29.76, 25.11.

4.1.6.2. Diethyl ((1R,1'R)-((2S,2'S)-(([1,1'-biphenyl]-4,4'-diylbis(azanediyl))bis(carbonyl))bis(pyrrolidine-2,1-diyl))bis(2-oxo-1-phenylethane-2,1-diyl))dicarbamate (2)

Yellow semi-solid; yield: 20%; $C_{44}H_{48}N_6O_8$; LC/MS: $[M+H]^+$ = 789.35; purity 91%; ^{1}H-NMR (400 MHz, DMSO) δ 7.69 – 7.54 (m, 9H), 7.47 – 7.32 (m, 9H), 5.73 (s, 2H), 4.64 – 4.32 (m, 2H), 4.05 – 3.48 (m, 8H), 2.05 – 1.73 (m, 8H), 1.13 (t, J = 7.1 Hz, 6H); ^{13}C-NMR (101 MHz, DMSO) δ 168.83, 168.60, 156.31, 130.08, 129.66, 129.02, 128.82, 128.47, 127.87, 126.85, 119.86, 55.34, 31.72, 29.46, 26.99, 25.11, 22.53, 15.08.

4.1.6.3. Dibutyl((1R,1'R)-((2S,2'S)-(([1,1'-biphenyl]-4,4'-diylbis(azanediyl))bis(carbonyl))bis(pyrrolidine-2,1-diyl))bis(2-oxo-1-phenylethane-2,1-diyl))dicarbamate (3)

Yellow semi-solid; yield: 22%; $C_{48}H_{56}N_6O_8$; LC/MS: $[M+H]^+$ = 845.42; purity 91%; ^{1}H-NMR (400 MHz, DMSO) δ 7.90 – 7.39 (m, 10H), 7.39 – 7.27 (m, 8H), 5.76 (s, 2H), 4.98 – 4.37 (m, 4H), 4.03 – 3.93 (m, 8H), 3.28 – 2.69 (m, 4H), 1.37 – 1.25 (m, 10H), 1.24 – 0.9 (m, 6H); ^{13}C-NMR (101 MHz, DMSO) δ 172.54, 169.49, 156.44, 140.73, 138.16, 129.06, 128.77, 128.50, 128.08, 126.81, 120.01, 119.57, 70.27, 67.44, 64.27, 58.62, 55.36, 31.18, 30.41, 19.02, 14.07.

4.1.6.4. Diisobutyl((1R,1'R)-((2S,2'S)-(([1,1'-biphenyl]-4,4'-diylbis(azanediyl))bis(carbonyl))bis(pyrrolidine-2,1-diyl))bis(2-oxo-1-phenylethane-2,1-diyl))dicarbamate (4)

Yellow semi-solid; yield: 25%; $C_{48}H_{56}N_6O_8$; LC/MS: $[M+H]^+$ = 845.42; purity 91%; ^{1}H-NMR (400 MHz, DMSO) δ 7.71 – 7.62 (m, 9H), 7.45 – 7.37 (m, 9H), 5.49 (s, 2H), 4.57 – 4.39 (m, 2H), 3.75 (d, J = 6.4 Hz, 4H), 3.27 – 3.01 (m, 4H), 2.01 – 1.76 (m, 10H), 0.85 (d, J = 5.5 Hz, 12H); ^{13}C-NMR (101 MHz, DMSO) 170.68, 168.88, 165.08, 137.61, 129.04, 128.85, 128.49, 128.22, 126.80, 120.10, 109.74, 70.64, 61.18, 57.09, 55.33, 29.77, 28.03, 24.70, 19.32.

4.1.6.5. Dibenzyl((1R,1'R)-((2S,2'S)-(([1,1'-biphenyl]-4,4'-diylbis(azanediyl))bis(carbonyl))bis(pyrrolidine-2,1-diyl))bis(2-oxo-1-phenylethane-2,1-diyl))dicarbamate (5)

Yellow semi-solid; yield: 25%; $C_{54}H_{52}N_6O_8$; LC/MS: $[M+H]^+$ = 913.38; purity 92%; ^{1}H NMR (400 MHz, DMSO) δ 7.71 – 7.67 (m, 4H), 7.66 – 7.62 (m, 4H), 7.47 – 7.35 (m, 20H), 5.75 (s, 2H), 5.05 (s, 4H), 4.72 – 4.21 (m, 2H), 3.11 – 2.91 (m, 4H), 2.03 – 1.96 (m, 8H); ^{13}C-NMR (101 MHz, DMSO) δ 178.21, 162.30, 155.11, 130.11, 130.04, 129.82, 129.56, 129.43, 129.11, 129.03, 128.87, 128.79, 128.51, 128.23, 128.10, 70.24, 55.35, 31.74, 29.47, 27.00, 22.55.

4.1.6.6. Dimethyl ((1S,1'S)-((2S,2'S)-2,2'-(([1,1'-biphenyl]-4,4' diylbis(azanediyl))bis(carbonyl)) bis(pyrrolidine-2,1-diyl))bis(2-oxo-1-phenylethane-2,1-diyl))dicarbamate (6)

Yellow semi-solid; yield: 38%; $C_{42}H_{44}N_6O_8$; LC/MS: $[M+H]^+$ = 761.59; purity 98.83%; ^{1}H-NMR (400 MHz, DMSO) δ 10.14 (s, 2H), 7.68 (d, J = 9.1 Hz, 4H), 7.63 (d, J = 3.4 Hz, 4H), 7.46 (d, J = 7.4 Hz, 4H), 7.38 (t, J = 3.7 Hz, 6H), 4.53 (dd, J = 8.2, 4.7 Hz, 2H), 3.55 (s, 8H), 3.17 (dd, J = 13.2, 7.0 Hz, 2H), 2.18 (dd, J = 18.5, 7.9 Hz, 2H), 1.94 – 1.79 (m, 8H); ^{13}C-NMR (101 MHz, DMSO) δ 170.75, 167.39, 158.42, 138.76,137.44, 134.52, 128.81, 127.99, 126.72, 119.64, 78.70, 61.23,59.02, 57.94, 48.33, 31.02, 24.05.

4.1.6.7. Diethyl ((1S,1'S)-((2S,2'S)-2,2'-(([1,1'-biphenyl]-4,4'-diylbis(azanediyl))bis(carbonyl)) bis(pyrrolidine-2,1-diyl))bis(2-oxo-1-phenylethane-2,1-diyl))dicarbamate (7)

Light yellow semi-solid; yield: 30%; $C_{44}H_{48}N_6O_8$; LC/MS: $[M+H]^+$ = 789.68; purity 92%; ^{1}H-NMR (400 MHz, DMSO) δ 10.12 (s, 2H), 7.61 (d, *J* = 9.6 Hz, 8H), 7.42 (d, *J* = 6.9 Hz, 4H), 7.34 (t, *J* = 9.4 Hz, 6H), 5.51 – 5.42 (m, 2H), 4.50 (s, 2H), 3.97 (d, *J* = 6.5 Hz, 4H), 3.09 (dd, *J* = 8.3, 5.8 Hz, 2H), 2.16 (dd, *J* = 10.7, 6.8 Hz, 2H), 1.88 – 1.82 (m, 4H), 1.21 (s, 4H), 1.13 (t, *J* = 6.9 Hz, 6H); ^{13}C-NMR (101 MHz, DMSO) δ 170.75, 168.39, 156.42, 138.86, 137.44, 134.82, 128.81, 128.06, 126.88, 119.64, 79.70, 61.19, 60.02, 56.94, 47.34, 30.00, 25.05, 15.20.

4.1.6.8. Dibutyl ((1S,1'S)-((2S,2'S)-2,2'-(([1,1'-biphenyl]-4,4'-diylbis(azanediyl))bis(carbonyl)) bis(pyrrolidine-2,1-diyl))bis(2-oxo-1-phenylethane-2,1-diyl))dicarbamate (8)

Light green semi-solid; yield: 23%; $C_{48}H_{56}N_6O_8$; LC/MS: $[M+H]^+$ = 845.74; purity 94%; ^{1}H-NMR (400 MHz, DMSO) δ 10.14 (s, 2H), 7.67 (s, *J* = 8.8 Hz, 4H), 7.58 (d, *J* = 8.4 Hz, 4H), 7.45 (d, *J* = 7.1 Hz, 4H), 7.39 – 7.34 (m, 6H), 5.48 (s, 2H), 4.53 (dd, *J* = 8.0, 4.5 Hz, 2H), 3.96 (t, *J* = 5.9 Hz, 4H), 3.14 (dd, *J* = 11.1, 3.9 Hz, 2H), 2.17 (dd, *J* = 12.0, 6.5 Hz, 2H), 1.91 – 1.85 (m, 4H), 1.55 – 1.49 (m, 4H), 1.36 – 1.24 (m, 8H), 0.89 (t, *J* = 7.2 Hz, 6H); ^{13}C-NMR (101 MHz, DMSO) δ 171.02, 169.59, 157.22, 139.56, 138.44, 135.88, 129.00, 128.08, 125.48, 120.10, 77.70, 62.29, 61.02, 57.55, 48.24, 32.02, 24.05, 19.98, 15.00, 14.07.

4.1.6.9. Diisobutyl ((1S,1'S)-((2S,2'S)-2,2'-(([1,1'-biphenyl]-4,4'-diylbis(azanediyl))bis(carbonyl)) bis(pyrrolidine-2,1-diyl))bis(2-oxo-1-phenylethane-2,1-diyl))dicarbamate (9)

Light green semi-solid; yield: 28%; $C_{48}H_{56}N_6O_8$; LC/MS: $[M+H]^+$ = 845.74; purity 100%; ^{1}H-NMR (400 MHz, DMSO) δ 10.16 (s, 2H), 7.66 (d, *J* = 8.7 Hz, 4H), 7.62 (d, *J* = 9.0 Hz, 4H), 7.46 (d, *J* = 7.3 Hz, 4H), 7.38 (t, *J* = 7.2 Hz, 6H), 5.50 (s, 2H), 4.53 (dd, *J* = 7.5, 4.4 Hz, 2H), 3.74 (d, *J* = 6.1 Hz, 4H), 3.15 (dd, *J* = 36.1, 8.8 Hz, 2H), 2.18 (dd, *J* = 19.0, 12.7 Hz, 2H), 1.96 – 1.76 (m, 8H), 1.29 – 1.20 (m, 2H), 0.88 (d, *J* = 6.7 Hz, 12H); ^{13}C-NMR (101 MHz, DMSO) δ 170.06, 169.00, 158.32, 139.00, 137.44, 134.00, 128.88, 127.05, 124.48, 121.13, 78.70, 64.33, 62.02, 58.23, 46.24, 29.89, 25.10, 18.98, 14.00.

4.1.6.10. Dibenzyl ((1S,1'S)-((2S,2'S)-2,2'-(([1,1'-biphenyl]-4,4'-diylbis(azanediyl))bis(carbonyl)) bis(pyrrolidine-2,1-diyl))bis(2-oxo-1-phenylethane-2,1-diyl))dicarbamate (10)

Yellow semi-solid; yield: 30%; $C_{54}H_{52}N_6O_8$; LC/MS: $[M+H]^+$ = 913.59; purity 96%; ^{1}H-NMR (400 MHz, DMSO) δ 10.11 (s, 2H), 7.61 (dd, *J* = 17.4, 7.9 Hz, 10H), 7.31 (dd, *J* = 18.7, 7.2 Hz, 18H), 5.50 (s, 2H), 5.02 (s, 4H), 4.50 (dd, *J* = 7.7, 4.9 Hz, 2H), 3.10 (dd, *J* = 15.5, 7.1 Hz, 2H), 2.16 (dd, *J* = 15.3, 8.2 Hz, 2H), 2.04 – 1.91 (m, 4H), 1.89 – 1.83 (m, 4H); ^{13}C-NMR (101 MHz,

DMSO) δ 171.94, 170.75, 168.63, 156.41, 144.67, 137.44, 128.84, 128.76, 128.20, 128.09, 119.84, 65.94, 60.97, 57.17, 29.52, 27.04, 23.63, 22.85, 14.35, 11.27, 10.59.

4.1.6.11.Dimethyl((2R,2'R)-((2S,2'S)-(([1,1'-biphenyl]-4,4'-diylbis(azanediyl))bis(carbonyl)) bis(pyrrolidine-2,1-diyl))bis(4-(methylthio)-1-oxobutane-1,2-diyl))dicarbamate (11)

Yellow semi-solid; yield: 30%; $C_{36}H_{48}N_6O_8S_2$; LC/MS: $[M+H]^+$ =757.30; purity 91%;^{1}H-NMR (400 MHz, DMSO) δ 7.70 – 7.63 (m, 8H), 4.50 – 4.41 (m, 4H), 3.58 (s, 6H), 3.56 – 3.53 (m, 4H), 2.88 (t, J = 8.2 Hz, 4H), 2.07 (s, 6H), 2.00 – 1.80 (m, 12H); ^{13}C-NMR (101 MHz, DMSO) δ 170.76, 157.24, 134.69, 130.60, 124.68, 114.94, 112.22, 55.24, 52.11, 34.91, 31.04, 30.08, 24.77, 22.59, 15.07, 14.85.

4.1.6.12. Diethyl((2R,2'R)-((2S,2'S)-(([1,1'-biphenyl]-4,4'-diylbis(azanediyl))bis(carbonyl))bis(pyrrolidine-2,1-diyl))bis(4-(methylthio)-1-oxobutane-1,2-diyl))dicarbamate (12)

Yellow semi-solid; yield: 20%; $C_{38}H_{52}N_6O_8S_2$; LC/MS: $[M+H]^+$ =785.33; purity 91%; ^{1}H-NMR (400 MHz, DMSO) δ 7.69 – 7.60 (m, 8H), 4.49 – 4.36 (m, 4H), 4.03 (q, J = 12.5 Hz, 4H), 3.82 – 3.48 (m, 4H), 2.71 – 2.68 (m, 4H), 2.06 (s, 6H), 2.00 – 1.74 (m, 12H), 1.16 (t, J = 7.0 Hz, 6H); ^{13}C-NMR (101 MHz, DMSO) δ 171.40, 170.76, 156.79, 138.45, 134.89, 126.81, 119.99, 61.04, 60.62, 55.34, 51.93, 47.31, 31.08, 30.10, 24.80, 22.60, 15.04.

4.1.6.13. Dibutyl((2R,2'R)-((2S,2'S)-(([1,1'-biphenyl]-4,4'-diylbis(azanediyl))bis(carbonyl))bis(pyrrolidine-2,1-diyl))bis(4-(methylthio)-1-oxobutane-1,2-diyl))dicarbamate (13)

Yellow semi-solid; yield: 30%; $C_{42}H_{60}N_6O_8S_2$; LC/MS: $[M+H]^+$ = 841.39; purity 96%; ^{1}H-NMR (400 MHz, DMSO) δ 7.86 – 7.25 (m, 8H), 4.43 (m, 4H), 3.99 – 3.95 (m, 4H), 3.84 – 3.57 (m, 4H), 2.57 – 2.53 (m, 4H), 2.06 (s, 6H), 1.94 – 1.74 (m, 12H), 1.51 (m, 8H), 0.85 (t, J = 4.8 Hz, 6H); ^{13}C-NMR (101 MHz, DMSO) δ 171.41, 170.82, 156.93, 138.45, 135.46, 126.84, 120.04, 64.36, 61.05, 51.97, 31.14, 30.26, 27.00, 24.78, 22.55, 19.01, 15.14, 14.86, 14.04.

4.1.6.14. Diisobutyl ((2R,2'R)-((2S,2'S)-(([1,1'-biphenyl]-4,4'-diylbis(azanediyl))bis(carbonyl))bis(pyrrolidine-2,1-diyl))bis(4-(methylthio)-1-oxobutane-1,2-diyl))dicarbamate (14)

Yellow semi-solid; yield: 21%;$C_{42}H_{60}N_6O_8S_2$; LC/MS: $[M+H]^+$ = 841.39; purity 91%; ^{1}H-NMR (400 MHz, DMSO) δ 7.70 – 7.50 (m, 8H), 4.46 – 4.39 (m, 2H), 4.13 – 3.94 (m, 2H), 3.73 – 3.69 (m, 8H), 2.20 – 2.04 (m, 8H), 2.01 (s, 6H), 1.84 – 1.76 (m, 8H), 1.24 – 1.09 (m, 2H), 0.85 (d, J = 2.8 Hz, 12H); ^{13}C-NMR (101 MHz, DMSO) δ 174.22, 170.81, 156.89, 138.63, 134.79, 126.80, 119.81, 70.30, 60.64, 53.08, 51.72, 47.36, 30.82, 30.25, 28.10, 25.13, 19.31, 14.92.

4.1.6.15.Dibenzyl((2R,2'R)-((2S,2'S)-(([1,1'-biphenyl]-4,4'-diylbis(azanediyl))bis(carbonyl)) bis(pyrrolidine-2,1-diyl))bis(4-(methylthio)-1-oxobutane-1,2-diyl))dicarbamate (15)

Off-white semi-solid; yield: 32%; $C_{48}H_{56}N_6O_8S_2$; LC/MS: $[M+H]^+$ = 909.36; purity 97%; ^{1}H-NMR (400 MHz, DMSO)δ 7.80 – 7.69 (m, 9H), 7.62 – 7.55 (m, 9H), 5.02 (s, 4H), 4.54 – 4.40 (m, 4H), 4.23 – 4.06 (m, 4H), 2.43 – 2.19 (m, 4H), 2.06 (s, 6H), 2.01 – 1.78 (m, 12H); ^{13}C-NMR (101 MHz, DMSO) δ 170.72, 167.42, 156.62, 137.33, 132.19, 131.99, 129.09, 128.78, 128.15, 126.77, 120.03, 67.84, 66.05, 55.42, , 30.27, 28.83, 23.71, 22.86, , 14.32, 11.23.

4.1.6.16.Dimethyl((2S,2'S)-((2S,2'S)-(([1,1'-biphenyl]-4,4'-diylbis(azanediyl))bis(carbonyl)) bis(pyrrolidine-2,1-diyl))bis(4-(methylthio)-1-oxobutane-1,2-diyl))dicarbamate (16)

Yellow semi-solid; yield: 35% ; $C_{36}H_{48}N_6O_8S_2$; LC/MS: $[M+H]^+$ = 757.30; purity 100%; ^{1}H-NMR (400 MHz, DMSO) δ 7.64 – 7.56 (m, 8H), 4.48 – 4.37 (m, 4H), 3.65 – 3.59 (m, 4H), 3.51 (s, 6H), 2.54 (t, J = 7.2 Hz, 4H), 2.05 (s, 6H), 1.98 – 1.72 (m, 12H); ^{13}C-NMR (101 MHz, DMSO) δ 170.83, 170.61, 157.04, 138.63, 134.78, 126.81, 119.84, 60.67, 55.28, 51.87, 47.39, , 31.16, 29.80, 25.10, 22.59, 15.09.

4.1.6.17. Diethyl((2S,2'S)-((2S,2'S)-(([1,1'-biphenyl]-4,4'-diylbis(azanediyl))bis(carbonyl))bis(pyrrolidine-2,1-diyl))bis(4-(methylthio)-1-oxobutane-1,2-diyl))dicarbamate (17)

Yellow semi-solid; yield: 33%; $C_{38}H_{52}N_6O_8S_2$; LC/MS: $[M+H]^+$ = 785.33; purity 100%; ^{1}H-NMR (400 MHz, DMSO) δ 7.66 – 7.55 (m, 8H), 4.42 (m, 4H), 3.96 (q, J = 7.0 Hz, 4H), 3.77 – 3.60 (m, 4H), 2.54 (t, J = 7.1 Hz, 4H), 2.04 (s, 6H), 1.98 – 1.70 (m, 12H), 1.13 (t, J = 3.5 Hz, 6H); ^{13}C-NMR (101 MHz, DMSO) δ 174.25, 170.82, 156.62, 138.63, 134.80, 126.81, 119.82, 60.31, 55.32, 53.03, 51.69, 47.37, 46.16, 31.11, 29.85, 25.13, 15.12.

4.1.6.18. Dibutyl((2S,2'S)-((2S,2'S)-(([1,1'-biphenyl]-4,4'-diylbis(azanediyl))bis(carbonyl))bis(pyrrolidine-2,1-diyl))bis(4-(methylthio)-1-oxobutane-1,2-diyl))dicarbamate (18)

Yellow semi-solid; yield:25%; $C_{42}H_{60}N_6O_8S_2$; LC/MS: $[M+H]^+$ = 841.39; purity 91%; ^{1}H-NMR (400 MHz, DMSO) δ 7.65 – 7.56 (m, 8H), 4.47 – 4.37 (m, 4H), 3.93 (t, J = 4.0 Hz, 4H), 3.77 – 3.64 (m, 4H), 2.54 (t, J = 7.8 Hz, 4H), 2.05 (s, 6H), 1.97 – 1.78 (m, 12H), 1.54 – 1.47 (m, 8H), 0.87 (t, J = 7.2 Hz, 6H); ^{13}C-NMR (101 MHz, DMSO) δ 174.20, 170.81, 156.73, 138.62, 134.81, 126.80, 119.83, 64.09, 60.64, 55.32, 53.13, 51.72, 47.36, 31.16, 29.86, 25.13, 19.01, 15.13, 14.04.

4.1.6.19. Diisobutyl((2S,2'S)-((2S,2'S)-(([1,1'-biphenyl]-4,4'-diylbis(azanediyl))bis(carbonyl))bis(pyrrolidine-2,1-diyl))bis(4-(methylthio)-1-oxobutane-1,2-diyl))dicarbamate (19)

Yellow semi-solid; yield: 26%; $C_{42}H_{60}N_6O_8S_2$; LC/MS: $[M+H]^+$ = 841.39; purity 92%; ^{1}H-NMR (400 MHz, DMSO) δ 7.65 – 7.56 (m, 8H), 4.52 – 4.39 (m, 4H), 4.05 (d, J = 4.7 Hz, 4H), 3.74 – 3.66 (m, 4H), 2.53 (t, J = 7.1 Hz, 4H), 2.01 (s, 6H), 1.97 – 1.85 (m, 2H), 1.85 – 1.77 (m, 12H), 0.85 (d, J = 2.8 Hz, 12H); ^{13}C NMR (101 MHz, DMSO) δ 174.22, 170.67, 156.89, 138.63, 134.79, 126.80, 119.81, 70.30, 60.64, 52.95, 51.77, 47.17, 30.82, 30.25, 28.10, 25.13, 19.31, 15.27.

4.1.6.20. Dibenzyl((2S,2'S)-((2S,2'S)-(([1,1'-biphenyl]-4,4'-diylbis(azanediyl))bis(carbonyl))bis(pyrrolidine-2,1-diyl))bis(4-(methylthio)-1-oxobutane-1,2-diyl))dicarbamate (20)

Off-white semi-solid; yield: 22%; $C_{48}H_{56}N_6O_8S_2$; LC/MS: $[M+H]^+$ = 909.36; purity 92%; ^{1}H-NMR (400 MHz, DMSO)δ 7.71 – 7.58 (m, 8H), 7.36 – 7.30 (m, 10H), 5.04 (s, 4H), 4.54 – 4.45 (m, 4H), 3.82 – 3.45 (m, 4H), 2.58 (t, J = 7.2 Hz, 4H), 2.06 (s, 6H), 2.04 – 1.80 (m, 12H); ^{13}C-NMR (101 MHz, DMSO) δ 173.09, 172.48, 170.81, 165.02, 156.51, 155.39, 142.95, 138.67, 137.42, 136.35, 134.87, 65.94, 63.40, 60.71, 55.32, 51.89, 47.43, 31.20, 29.89, 25.15.

4.1.6.21. Dimethyl ((2R,2'R)-((2S,2'S)-2,2'-(([1,1'-biphenyl]-4,4'-diylbis(azanediyl))bis(carbonyl)) bis(pyrrolidine-2,1-diyl))bis(3-(methylthio)-1-oxopropane-2,1-diyl))dicarbamate (21)

Yellowish white semi-solid; yield: 28.76%; $C_{34}H_{44}N_6O_8S_2$; LC/MS: $[M+H]^+$ = 729.49; purity 97%; ^{1}H-NMR (400 MHz, DMSO) δ 10.00 (s, 2H), 7.62 (d, *J* = 8.8 Hz, 4H), 7.58 (d, *J* = 6.4 Hz, 4H), 4.44 – 4.42 (m, 2H), 3.67 (d, *J* = 6.5 Hz, 2H), 3.53 (s, 6H), 2.80 (dd, *J* = 13.9, 4.5 Hz, 2H), 2.58 (d, *J* = 19.0 Hz, 4H), 2.16 (dd, *J* = 10.4, 5.4 Hz, 2H), 2.10 (s, 6H), 2.06 – 1.95 (m, 4H), 1.94 – 1.88 (m, 4H); ^{13}C-NMR (101 MHz, DMSO) δ 170.51, 169.02, 157.21, 138.14, 134.37, 126.33,119.86, 60.80, 52.42, 52.01, 47.41, 35.28, 29.92, 24.57, 14.63.

4.1.6.22. Diethyl ((2R,2'R)-((2S,2'S)-2,2'-(([1,1'-biphenyl]-4,4'-diylbis(azanediyl))bis(carbonyl)) bis(pyrrolidine-2,1-diyl))bis(3-(methylthio)-1-oxopropane-2,1-diyl))dicarbamate (22)

Yellow semi-solid; yield: 29%; $C_{36}H_{48}N_6O_8S_2$; LC/MS: $[M+H]^+$ = 757.52; purity 90%; ^{1}H-NMR (400 MHz, DMSO) δ 10.00 (s, 2H), 7.62 (d, *J* = 8.4 Hz, 4H), 7.57 (d, *J* = 8.1 Hz, 4H), 4.44 – 4.42 (m, 2H), 4.00 – 3.95 (m, 4H), 3.67 (d, *J* = 6.5 Hz, 2H), 2.79 (dd, *J* = 13.7, 3.9 Hz, 2H), 2.68 – 2.50 (m, 4H), 2.21 – 2.14 (m, 2H), 2.10 (s, 6H), 2.06 – 1.96 (m, 4H), 1.94 – 1.88 (m, 4H), 1.14 (t, *J* = 7.0 Hz, 6H); ^{13}C-NMR (101 MHz, DMSO) δ 170.65, 169.47, 156.59, 138.54, 134.81, 126.80, 119.92, 61.24, 60.22, 52.72, 47.30, 35.41, 29.66, 24.87, 15.57, 14.85.

4.1.6.23. Dibutyl ((2R,2'R)-((2S,2'S)-2,2'-(([1,1'-biphenyl]-4,4'-diylbis(azanediyl))bis(carbonyl)) bis(pyrrolidine-2,1-diyl))bis(3-(methylthio)-1-oxopropane-2,1-diyl))dicarbamate (23)

Greenish white semi-solid; yield: 30%; $C_{40}H_{56}N_6O_8S_2$; LC/MS: $[M+H]^+$ = 813.61; purity 92%; ^{1}H-NMR (400 MHz, DMSO) δ 9.98 (s, 2H), 7.62 (d, *J* = 8.8 Hz, 4H), 7.57 (d, *J* = 8.8 Hz, 4H), 4.43 (dd, *J* = 7.4, 3.2 Hz, 2H), 3.94 (t, *J* = 5.7 Hz, 4H), 3.70 – 3.65 (m, 2H), 2.79 (dd, *J* = 13.8, 4.4 Hz, 2H), 2.59 (d, *J* = 23.3 Hz, 4H), 2.15 (dd, *J* = 12.1, 8.5 Hz, 2H), 2.10 (s, 6H), 1.96 – 1.88 (m, 4H), 1.55 – 1.47 (m, 4H), 1.34 – 1.28 (m, 4H), 1.25 – 1.19 (m, 4H), 0.87 (t, *J* = 7.3 Hz, 6H); ^{13}C-NMR (101 MHz, DMSO) δ 170.76, 169.58, 156.89, 138.86, 135.07, 126.86, 120.12, 64.25, 60.94, 55.61, 52.53, 35.36, 31.18, 29.77, 25.04, 19.00, 15.91, 14.27.

4.1.6.24. Diisobutyl ((2R,2'R)-((2S,2'S)-2,2'-(([1,1'-biphenyl]-4,4'-diylbis(azanediyl))bis(carbonyl)) bis(pyrrolidine-2,1-diyl))bis(3-(methylthio)-1-oxopropane-2,1-diyl))dicarbamate (24)

Light green semi-solid; yield: 34%; $C_{40}H_{56}N_6O_8S_2$; LC/MS: $[M+H]^+$ = 813.61; purity 100%; ^{1}H-NMR (400 MHz, DMSO) δ 9.98 (s, 2H), 7.62 (s, 4H), 7.58 (s, 4H), 4.40 (d, *J* = 23.0 Hz, 4H), 3.73 (s, 4H), 3.62 (d, *J* = 35.2 Hz, 4H), 2.84 – 2.70 (m, 2H), 2.68 – 2.53 (m, 2H), 2.10 (s, 6H), 2.08 – 1.95 (m, 4H), 1.94 – 1.85 (m, 4H), 1.85 – 1.77 (m, 2H), 0.86 (s, 12H); ^{13}C-NMR (101 MHz, DMSO) δ 170.52, 169.73, 156.78, 138.54, 135.07, 126.32, 120.18, 70.33, 61.20, 52.37, 47.11, 34.89, 29.53, 27.63, 24.57, 19.61, 15.82.

4.1.6.25. Dibenzyl ((2R,2'R)-((2S,2'S)-2,2'-(([1,1'-biphenyl]-4,4'-diylbis(azanediyl))bis(carbonyl)) bis(pyrrolidine-2,1-diyl))bis(3-(methylthio)-1-oxopropane-2,1-diyl))dicarbamate (25)

Light brown semi-solid; yield: 26.5%; $C_{46}H_{52}N_6O_8S_2$; LC/MS: $[M+H]^+$ = 881.58; purity 93%; ^{1}H-NMR (400 MHz, DMSO) δ 10.00 (s, 2H), 7.62 (d, *J* = 8.7 Hz, 4H), 7.57 (d, *J* = 8.8 Hz, 4H), 7.36 – 7.31 (m, 10H), 5.03 (s, 4H), 4.45 (dd, *J* = 6.9, 2.7 Hz, 2H), 3.69 – 3.66 (m, 2H), 2.81 (dd, *J* = 13.9, 4.4 Hz, 2H), 2.60 (d, *J* = 23.3 Hz, 4H), 2.15 (dd, *J* = 10.9, 7.6 Hz, 2H), 2.10 (s, 6H), 2.06 – 1.94 (m, 4H), 1.93 – 1.86 (m, 4H); ^{13}C-NMR (101 MHz, DMSO) δ 170.57, 169.11, 156.36, 138.27,

137.29, 134.63, 128.79, 128.27, 128.16, 126.80, 119.70, 65.85, 60.70, 52.41, 47.24, 35.14, 29.98, 24.64, 15.82.

4.2. Biological studies

Huh5-2 [26] and Huh7-JFH1 [31] stable cell lines contained the subgenomic HCV reporter replicon I_{389}luc-ubi-neo/NS3-3'/Con1/5.1 (genotype 1b; strain Con1) and I_{389}luc-ubi-neo/NS3-3'_dg_JFH1 (genotype 2a, JFH1 strain), respectively (provided kindly by R. Bartenschlager, Heidelberg University, Germany). Huh7.5-3a and Huh7.5-4a stable cell lines [32] contain the subgenomic HCV reporter replicon S52-SG (Feo) (AII) (genotype 3a; S52 strain) and ED43-SG (Feo)(VYG) (genotype 4a; ED43 strain) [33], respectively (viral constructs provided kindly by C.M. Rice, The Rockefeller University, NY). These bicistronic replicons express firefly luciferase and neomycin phosphotransferase under the translational control of the HCV internal ribosome entry site (IRES) and HCV NS3 to NS5B proteins under the control of the EMCV IRES.

Cells cultured in high glucose (25 mM) Dulbecco's modified minimal essential medium (Invitrogen), supplemented with 2 mM L-glutamine, 0.1 mM non-essential amino acids, 100 U/mL penicillin, 100 µg/mL streptomycin and 10% (v/v) fetal calf serum (referred to as complete DMEM). Complete DMEM has been supplemented with 500 µg/mL G418 for Huh5-2, 1 mg/ml for Huh7-JFH1, 750 µg/ml G418 for Huh7.5-3a and 350 µg/mL G418 for Huh7.5-4a.

4.2.1. Cell-based antiviral and cytotoxicity assays

Antiviral and cytotoxicity assays were performed by seeding $1x10^4$ replicon cells per well in a 96-well flat bottom plate. Medium was exchanged with the serial dilutions of the synthesized compounds in complete DMEM. Compounds were then diluted in DMSO, such that the final concentration in complete DMEM was 0.2%. The cells were then cultured at 37°C (5% CO_2) and

lysed after 3 days. Viral replication levels were determined by measuring Firefly luciferase (F-Luc) activity and the cytotoxicity of the test compounds was determined by recording intracellular ATP levels, using the respective chemiluminescence-based assays. Relative luminescence units (RLU) were calculated as percentage relative to the respective values from DMSO-treated control cells.

The median effective concentration (EC_{50}) was determined as the concentration of compound that inhibited the luciferase signal by 50%, and median cytotoxic concentration (CC_{50}) was determined as the compound concentration leading to 50% cell death. EC_{50} and CC_{50} values were detected by nonlinear regression analysis after converting the drug concentrations into log-X using the Prism 5.0 software (GraphPad Software Inc.).

4.2.2. Luciferase and Bradford assays

Luciferase Assay System (Promega) was used to measure the Firefly luciferase activity in cell lysates, recommended by the manufacturer. Measurements were performed with a GloMax 20/20 single tube luminometer (Promega) for 10 seconds. F-Luc activity was normalized to the total intracellular protein level, detected by Bradford assay (Pierce).

4.2.3. Measurement of the levels of intracellular ATP

ATP levels were measured using the ViaLight HS BioAssay kit (Lonza) according to the protocol of the manufacturer in a GloMax 20/20 single-tube luminometer (Promega) for 1 second. ATP was normalized to the total protein amounts.

4.2.4. Indirect immunofluorescence

Indirect immunofluorescence analysis of Con1 NS5A was carried out as previously described elsewhere [34]. DNA was stained with propidium iodide (provided by Sigma-Aldrich) and the images were detected with the Leica TCS-SP8P Confocal Microscope.

4.2.5. Total RNA extraction and quantification of viral replicons

Total RNA was extracted using TRIzol reagent (Ambion) from Huh5-2 cells, according to the instructions of the manufacturer. The quantification of replicon RNA was performed with reverse-transcription (RT) and quantitative real-time polymerase chain reaction (qPCR). The Con1 IRES specific primer 5'-GGATTCGTGCTCATGGTGCA-3' (reverse) and Moloney Murine Leukemia Virus (MMLV) reverse transcriptase (Promega) were used for RT. The Con1 IRES specific primers 5'-GGCCTTGTGGTACTGCCTGATA-3' (forward) and 5'-GGATTCGTGCTCATGGTGCA-3' (reverse) and KAPA SYBR FAST qPCR Master Mix (Kapa Biosystems) were used for qPCR.

The housekeeping gene YWHAZ was used as normalization control (primers 5'-GCTGGTGATGACAAGAAAGG-3'and 5'- GGATGTGTTGGTTGCATTTCCT -3').

4.2.6. Statistical analysis

All diagrams, bars represented the mean values of at least two independent experiments in triplicate. The standard deviation was represented by error bars. The results subjected to statistical analysis using Student's t-test with $p \leq 0.05$ were considered as statistically significant and presented. The statistical calculations have been carried out using Excel Microsoft Office®.

Acknowledgement

The project is funded by the Science and Technology Development Fund (STDF), Egypt, Grant # 22848 to Ashraf Abadi.

References:

[1] World Health Organization, 2018, Hepatitis C http://www.who.int/mediacentre/factsheets/fs164/en/.
[2] P. Simmonds, P. Becher, J. Bukh, E.A. Gould, G. Meyers, T. Monath, S. Muerhoff, A. Pletnev, R. Rico-Hesse, D.B. Smith, J.T. Stapleton, ICTV Virus Taxonomy Profile: Flaviviridae, J. Gen. Virol. 98 (2017) 2-3, https://doi.org/10.1099/jgv.0.000672.
[3] V. Lohmann, R. Bartenschlager, On the History of Hepatitis C Virus Cell Culture Systems: Miniperspective, J. Med. Chem. 57 (2013) 1627-1642, https://*doi*.org/*10.1021/jm401401n.*
[4] K. Tsukiyama-Kohara, M. Kohara, Hepatitis C Virus: Viral Quasispecies and Genotypes, Int. J. Mol. Sci. 19 (2017) 23, https://doi.org/10.3390/ijms19010023.
[5] R. Bartenschlager, V. Lohmann, F. Penin, The molecular and structural basis of advanced antiviral therapy for hepatitis C virus infection, Nat. Rev. Microbiol. 11 (2013) 482-496, https://doi.org/10.1038/nrmicro3046.
[6] D. Moradpour, F. Penin, C.M. Rice, Replication of hepatitis C virus, Nat. Rev. Microbiol. 5 (2007) 453-463, https://doi.org/10.1038/nrmicro1645.
[7] D. Ross-Thriepland, M. Harris, Hepatitis C virus NS5A: enigmatic but still promiscuous 10 years on! J. Gen. Virol. 96 (2015) 727-738, https://doi.org/10.1099/jgv.0.000009.
[8] J.-M. Pawlotsky, Hepatitis C virus: standard-of-care treatment, Adv. Pharmacol. Elsevier. 67 (2013) 169-215, https://doi.org/10.1016/B978-0-12-405880-4.00005-6.
[9] P.W. Hofmann, S. Zeuzem, A new standard of care for the treatment of chronic HCV infection, Nat. Rev. Gastroenterol. Hepatol. 8 (2011) 257-264, https://doi.org/10.1038/nrgastro.2011.49.
[10] A.B. Jazwinski, A.J. Muir, Direct-acting antiviral medications for chronic hepatitis C virus infection, Gastroenterol. Hepatol. 7 (2011) 154-162, https://www.ncbi.nlm.nih.gov/pubmed/21528041.
[11] G. Li, E. De Clercq, Current therapy for chronic hepatitis C: The role of direct-acting antivirals, Antiviral Res. 142 (2017) 83-122, https://doi.org/10.1016/j.antiviral.2017.02.014.
[12] J.M. Gottwein, L.V. Pham, L.S. Mikkelsen, L. Ghanem, S. Ramirez, T.K.H. Scheel, T.H.R. Carlsen, J. Bukh, Efficacy of NS5A Inhibitors Against Hepatitis C Virus Genotypes 1-7 and Escape Variants, Gastroenterology. 154 (2018) 1435-1448, https://doi.org/10.1053/j.gastro.2017.12.015.
[13] A.R.S. Leila, M.H.A. Mousa, E. Frakolaki, N. Vassilaki, R. Bartenschlager, G. Zoidis, M. Abdel-Halim, A.H. Abadi, Symmetric Anti-HCV Agents: Synthesis, Antiviral Properties and Conformational Aspects of Core Scaffolds, ACS Omega 4 (2019) 11440-11454, https://doi.org/10.1021/acsomega.9b01242.
[14] C. Wang, L. Jia, D.R. O'Boyle, J.H. Sun, K. Rigat, L. Valera, P. Nower, X. Huang, B. Kienzle, S. Roberts, M. Gao, R.A. Fridell, Comparison of daclatasvir resistance barriers on NS5A from hepatitis C virus genotypes 1 to 6: implications for cross-genotype activity, Antimicrob. Agents Chemother. 58 (2014) 5155-6, https://doi.org/10.1128/AAC.02788-14.

[15] V. Gimeno-Ballester, M. Buti, R. San Miguel, M. Riveiro, R. Esteban, Interferon-free therapies for patients with chronic hepatitis C genotype 3 infection: A systematic review, J. Viral Hepat. 24 (2017) 904-916, https://doi.org/10.1111/jvh.12660.
[16] J.O. Link, J.G. Taylor, L. Xu, M. Mitchell, H. Guo, H. Liu, D. Kato, T. Kirschberg, J. Sun, N. Squires, J. Parrish, T. Kellar, Z.Y. Yang, C. Yang, M. Matles, Y. Wang, K. Wang, G. Cheng, Y. Tian, E. Mogalian, E. Mondou, M. Cornpropst, J. Perry, M.C. Desai, Discovery of ledipasvir (GS-5885): a potent, once-daily oral NS5A inhibitor for the treatment of hepatitis C virus infection, J. Med. Chem. 57 (2014) 2033-2046, https://doi.org/10.1021/jm401499g.
[17] T.M. Ramsis, S.E. Abdelkarim, N. Vassilaki, E. Frakolaki, A.A. Kamal, G. Zoidis, N.S. Ahmed, A.H. Abadi, Expanding the chemical space of anti-HCV NS5A inhibitors by stereochemical exchange and peptidomimetic approaches, Archiv. der Pharmazie 351 (2018) 1-10, https://doi.org/10.1002/ardp.201800017.
[18] S.M. Lambert, D.R. Langley, J.A. Garnett, R. Angell, K. Hedgethorne, N.A. Meanwell, S.J. Matthews, The crystal structure of NS5A domain 1 from genotype 1a reveals new clues to the mechanism of action for dimeric HCV inhibitors, Protein Sci. 23 (2014) 723-734, https://doi.org/10.1002/pro.2456.
[19] D. Cordek, J. Bechtel, A. Maynard, W. Kazmierski, C. Cameron, Targeting the NS5A protein of HCV: an emerging option, Drugs Future 36 (2011) 691-711, https://doi.org/10.1358/dof.2011.036.09.1641618.
[20] T.L. Tellinghuisen, J. Marcotrigiano, C.M. Rice, Structure of the zinc-binding domain of an essential component of the hepatitis C virus replicase, Nature 435 (2005) 374-379, https://doi.org/10.1038/nature03580.
[21] J.H. Nettles, R.A. Stanton, J. Broyde, F. Amblard, H. Zhang, L. Zhou, J. Shi, T.R. McBrayer, T. Whitaker, S.J. Coats, J.J. Kohler, R.F. Schinazi, Asymmetric binding to NS5A by daclatasvir (BMS-790052) and analogs suggests two novel modes of HCV inhibition, J. Med. Chem. 57 (2014) 10031-10043, https://doi.org/10.1021/jm501291c.
[22] D.B. Ascher, J. Wielens, T.L. Nero, L. Doughty, C.J. Morton, M.W. Parker, Potent hepatitis C inhibitors bind directly to NS5A and reduce its affinity for RNA, Sci. Rep. 4 (2014) 4765, https://doi.org/10.1038/srep04765.
[23] Y.A. Ivanenkov, M.S. Veselov, V.A. Aladinskiy, A.G. Shakhbazyan, S.M. Yartseva, A.G. Majouga, A.V. Aladinskaya, A.S. Vantskul, S.V. Leonov, A.V. Ivachtchenko, V.E. Koteliansky, In silico approaches to the design of NS5A inhibitors, Curr. Top. Med. Chem. 16 (2016) 1383-1391, https://doi.org/10.2174/1568026616666151120113705.
[24] K.H. Barakat, A. Anwar-Mohamed, J.A. Tuszynski, M.J. Robins, D.L. Tyrrell, M. Houghton, A refined model of the HCV NS5A protein bound to daclatasvir explains drug-resistant mutations and activity against divergent genotypes, J. Chem. Inf. Model. 55 (2014) 362-373, https://doi.org/10.1021/ci400631n.
[25] S. Boucle, S. Tao, F. Amblard, R.A. Stanton, J.H. Nettles; C. Li, T.R. McBrayer, T. Whitaker, S.J. Coats, R.F. Schinazi, Design, synthesis and evaluation of novel anti-HCV molecules that deliver intracellularly three highly potent NS5A inhibitors, Bioorg. Med. Chem. Lett. 25 (2015) 3711-3715, https://doi.org/10.1016/j.bmcl.2015.06.031.
[26] J.M. Vrolijk, A. Kaul, B.E. Hansen, V. Lohmann, B.L. Haagmans, S.W. Schalm, R. Bartenschlager, A replicon-based bioassay for the measurement of interferons in patients with chronic hepatitis C, J. Virol. Methods. 110 (2003) 201-209, https://doi.org/10.1016/s0166-0934(03)00134-4.
[27] K.M. Engle, D.-H. Wang, J.-Q. Yu, Ligand-accelerated C−H activation reactions: evidence for a switch of mechanism, J. Am. Chem. Soc. 132 (2010) 14137-14151, https://doi.org/10.1021/ja105044s.
[28] M. Włostowski, S. Czarnocka, P. Maciejewski, Efficient S-alkylation of cysteine in the presence of 1,1,3,3-tetramethylguanidine, Tetrahedron Lett. 51 (2010) 5977-5979, https://doi.org/10.1016/j.tetlet.2010.09.014.
[29] D.R. St. Laurent, M.H. Serrano-Wu, M. Belema, M. Ding, H. Fang, M. Gao, J.T. Goodrich, R.G. Krause, J.A. Lemm, M. Liu, O.D. Lopez, V.N. Nguyen, P.T. Nower, D.R. O'Boyle, B.C. Pearce, J.L. Romine, L.

Valera, J.H. Sun, Y.K. Wang, F. Yang, X. Yang, N.A. Meanwell, L.B. Snyder, HCV NS5A Replication Complex Inhibitors. Part 4. Optimization for Genotype 1a Replicon Inhibitory Activity, J. Med. Chem. 57 (2013) 1976-1994, https://doi.org/10.1021/jm301796k.

[30] H.I. Bae, J.K. Choi, C. Chough, S.J. Keum, H. Kim, S.K. Jang, B.M. Kim, Potent hepatitis C virus NS5A inhibitors containing a benzidine core, ACS Med. Chem. Lett. 5 (2013) 255-258, https://doi.org/10.1021/ml4003293.

[31] J. Jo, U. Aichele, N. Kersting, R. Klein, P. Aichele, E. Bisse, A.K. Sewell, H.E. Blum, R. Bartenschlager, V. Lohmann, R. Thimme, Analysis of CD8+ T-cell-mediated inhibition of hepatitis C virus replication using a novel immunological model, Gastroenterology. 136 (2009) 1391-1401, https://doi.org/10.1053/j.gastro.2008.12.034.

[32] E. Giannakopoulou, V. Pardali, E. Frakolaki, V. Siozos, V. Myrianthopoulos, E. Mikros, M.C. Taylor, J.M. Kelly, N. Vassilaki, G. Zoidis, Scaffold hybridization strategy towards potent hydroxamate-based inhibitors of Flaviviridae viruses and Trypanosoma species, MedChemCom. 10 (2019) 991-1006, https://doi.org/10.1039/c9md00200f.

[33] M. Saeed, T.K. Scheel, J.M. Gottwein, S. Marukian, L.B. Dustin, J. Bukh, C.M. Rice, Efficient replication of genotype 3a and 4a hepatitis C virus replicons in human hepatoma cells, Antimicrob. Agents Chemother. 56 (2012) 5365-5373, https://doi.org/10.1128/AAC.01256-12.

[34] N. Vassilaki, P. Friebe, P. Meuleman, S. Kallis, A. Kaul, G. Paranhos-Baccala, G. Leroux-Roels, P. Mavromara, R. Bartenschlager, Role of the hepatitis C virus core+1 open reading frame and core cis-acting RNA elements in viral RNA translation and replication, J. Virol. 82 (2008) 11503-15, https://doi.org/10.1128/JVI.01640-08.

Graphical Abstract

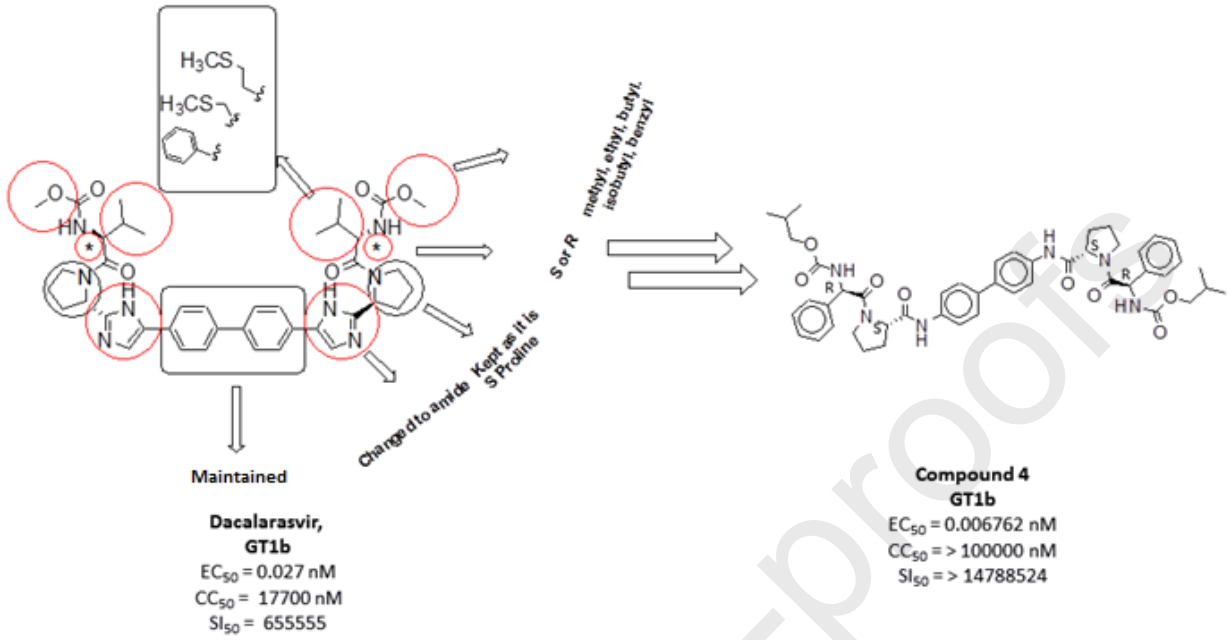

Highlights

The manuscript highlights are:

1. Twenty five compounds were synthesized and structurally elucidates.
2. Several compounds showed EC50s in the picomolar or nanomolar range against genotype 1b
3. Several compounds showed high selectivity indices up to 7 orders of magnitude.
4. Active molecules are with unnatural amino acids, amino acids other than valine and with carbamates other than methyl.
5. The activity and safety profiles of several respective compounds were better than the clinical candidate Daclatasvir.
6. This enlarges the chemical space from which NS5A inhibitors may be discovered.